51. IWK

Internationales Wissenschaftliches Kolloquium
International Scientific Colloquium

PROCEEDINGS 11-15 September 2006

FACULTY OF ELECTRICAL ENGINEERING AND INFORMATION SCIENCE

INFORMATION TECHNOLOGY AND ELECTRICAL ENGINEERING - DEVICES AND SYSTEMS, MATERIALS AND TECHNOLOGIES FOR THE FUTURE

Startseite / Index:
http://www.db-thueringen.de/servlets/DocumentServlet?id=12391

TECHNISCHE UNIVERSITÄT
ILMENAU

Impressum

Herausgeber: Der Rektor der Technischen Universität Ilmenau
Univ.-Prof. Dr. rer. nat. habil. Peter Scharff

Redaktion: Referat Marketing und Studentische Angelegenheiten
Andrea Schneider

Fakultät für Elektrotechnik und Informationstechnik
Susanne Jakob
Dipl.-Ing. Helge Drumm

Redaktionsschluss: 07. Juli 2006

Technische Realisierung (CD-Rom-Ausgabe):
Institut für Medientechnik an der TU Ilmenau
Dipl.-Ing. Christian Weigel
Dipl.-Ing. Marco Albrecht
Dipl.-Ing. Helge Drumm

Technische Realisierung (Online-Ausgabe):
Universitätsbibliothek Ilmenau
ilmedia
Postfach 10 05 65
98684 Ilmenau

Verlag:
Verlag ISLE, Betriebsstätte des ISLE e.V.
Werner-von-Siemens-Str. 16
98693 Ilrnenau

ISBN (Druckausgabe): 3-938843-15-2
ISBN (CD-Rom-Ausgabe): 3-938843-16-0

Startseite / Index:
http://www.db-thueringen.de/servlets/DocumentServlet?id=12391

51st Internationales Wissenschaftliches Kolloquium
Technische Universität Ilmenau
September 11 – 15, 2006

Precise Temperature and Force Sensing with Quartz Thickness-Shear Resonators

1. Valahia University of Targoviste,
B-dul Unirii Nr. 18-20, Târgovişte 130082,
ROMANIA
Phone: +40 723 06 00 46
Fax: +40 245 21 76 83
E-mail: ivan@valahia.ro, cimpoca@valahia.ro

2. FEMTO-ST/ Dept. LCEP, ENSMM,
26 Chemin de l'Epitaphe, Besançon 25030,
FRANCE
Phone: +333 81 40 28 22
Fax: +333 81 88 57 14
E-mail: aivan@ens2m.fr, rbourquin@ens2m.fr

***Abstract* – This paper presents a microprocessor-based distributed system architecture designed to interconnect piezoelectric resonant sensors to a measurement and control unit.**

Previously, a multielectrode (ME) temperature compensated force sensor was designed and prototyped, featuring thickness-shear dual mode operation driven by several pairs of electrodes, as seen in published article [1]. The starting idea to design the resonator was to optimize a particular electrodes shape that could allow dual mode excitation by electrically isolated electronic oscillators. This approach greatly simplified the electronics, knowing that dual mode operation with classical electrodes requires elaborate schematics for signal mixing and filtering to finally discriminate the vibrating mode frequencies. In our case, since the signals are already separated, only a minimal attention was paid to design of electronic oscillators, the rest of the work being devoted to frequency counting and information processing.

Quartz thermosensitive (QT) resonators is a family of miniaturized thickness-shear resonators developed under a joint European project collaboration called QxSens [7],[8]. These sensors offer a large measurement range down to cryogenic temperatures, providing at the same time resolutions below the miliKelvin.

The present paper continues the work and focuses over the electronic device necessary for extracting the useful output data from raw frequency values provided by these two types of sensors.

1 INTRODUCTION ON MULTIELECTRODE (ME) RESONATOR FEATURES

The force sensitive element is a plano-convex disk-shaped thickness-shear resonator manufactured in quartz. The diameter of the plate is 13.2 mm, the curvature radius of the convex side is 300mm while the thickness of the plate is 0.7 mm. The quartz crystal had an SC-cut [2]. Electrodes were made by vacuum deposition of gold over a chrome layer followed by photolithography. Resulted plates were tested extensively [1] under different force and temperature conditions. The design of electrodes is not a subject of the paper, although it should be stressed out that a good concordance was found between analytical simulation of vibrating amplitude distribution and experimental X-rays topographies [1,6] performed on the real samples.

One vibrating mode (so-called C-mode) is mainly sensitive both to a compressional diametral force and to the temperature, while the other mode (B-mode) is about fifty times more sensitive to the temperature and almost insensitive to the applied force.

Figure 1-2 explains the geometry of the resonator plate while figures 3.a,b,c shows several pictures of the first series of prototypes.

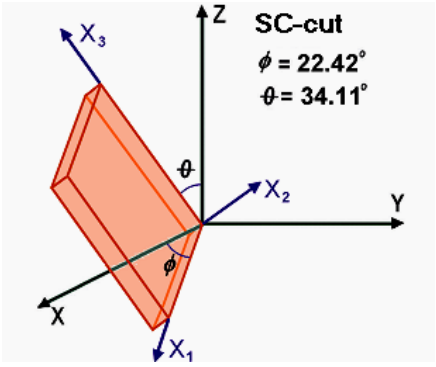

Figure 1. SC-Cut in quartz. (XYZ) represents crystalline system of axis and ($X_1X_2X_3$) is the cut coordinates system

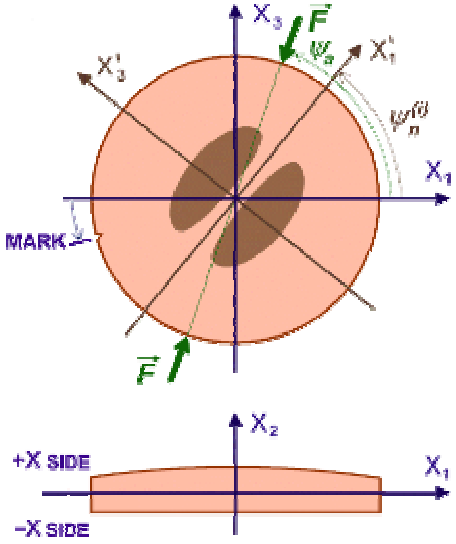

Figure 2. SC-Cut resonator geometry. $(X_1'X_2'X_3')$ is the local mode system of axis turned by the angle ψ_n w.r.t. $(X_1X_2X_3)$. The external force F is applied at ψ_a azimuth angle.

The mark in Figure 3 is made during manufacturing of plate for orientation purposes and represents the projection of the crystallographic axis –X over the (X_1X_3) plane of the cut. The value of the turning angle is 13^0.

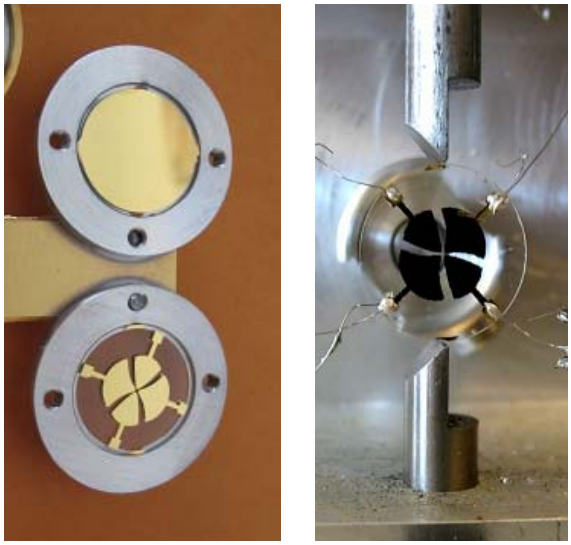

Figure 3.a) Plate completely metalized by vacuum deposition
b) Plate after UV photolithography
c) Resonator with electrical connections under compressional force setup.

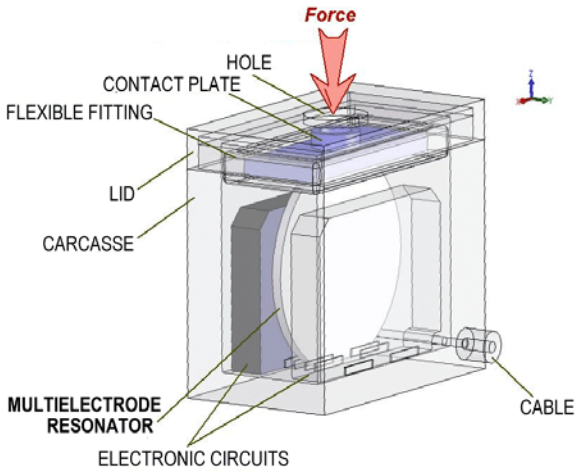

Figure 3.d) Future project of a complete transducer encapsulating resonator and relied electronics

The possibility to integrate the ME resonator and relied electronics (oscillators plus digital conversion unit) has been studied and is in feasible, as seen in figure 3.d.

2 MULTIELECTRODE TRANSFER EQUATIONS SET

This part discusses electrical equivalent schematic and motional parameters values necessary to design the electronic oscillators. Afterwards it presents experimental results from testing the first prototypes and establishes the method to compute the force and temperature based on the two resonant frequencies of B and C modes.

2.1 Equivalent electrical schematic

The first series of samples were tested in a passive PI network, in order to calculate the equivalent electrical parameters, according to the schematic shown in figure 4.

Quality factors Q of the resonators were found to be equal with 211037 and 120800 respectively. Motional resistances R_1 range around 20…30 kΩ, inductances L_1 around 55…90 H, and equivalent dynamic capacitances C_1 equal about 0,005 fF as seen in the table below.

Pairs of electrodes are named according to paper [1] notation. Static parallel capacitance Co of the pair P2+P4 intended to work for the C-mode is 3,1 pF and the value of static capacitance of the B-mode pair P1+P3 is equal to 2,7 pF.

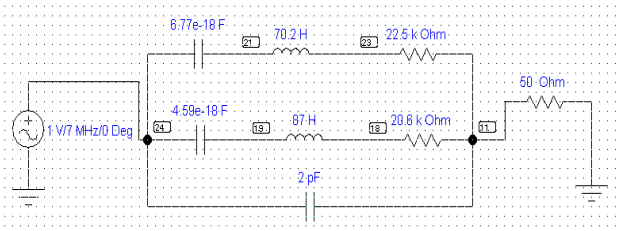

Figure 4. Electrical equivalent schematic – electrodes pair P2+P4 [1].

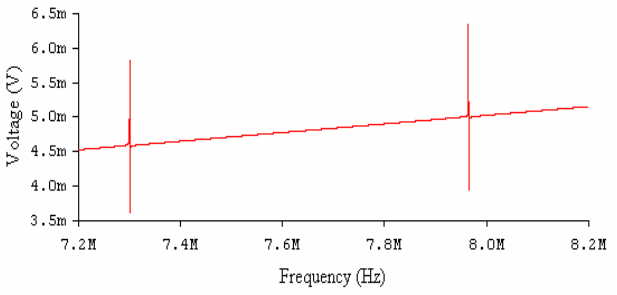

Figure 4. Frequency analysis simulation.

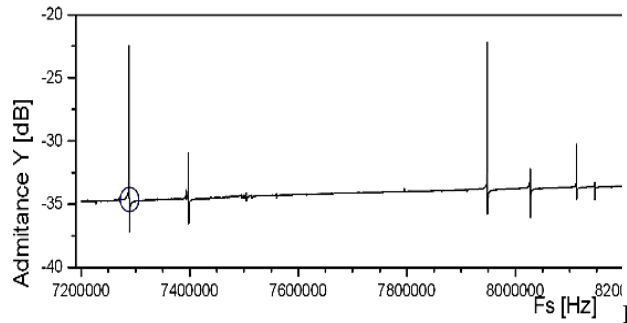

Figure 5. Experimental frequency spectrum

The operating frequency for this pair of electrodes (P2+P4) is marked by a circle in figure 5. The rest of the modes are unwanted ones and can be further suppressed by the electronic oscillator.

2.2 Frequency to temperature experimental characteristics

Frequencies – temperature curves of the resonators were investigated under a controlled oven between –15 ^{0}C and +90 ^{0}C. However, experiments can be performed over a wider temperature range. As known, mode B offers large temperature sensitivity, with a fairly linear slope. The C-mode is temperature compensated, exhibiting a cubic frequency to temperature curve. We fitted the experimental data under different polynomials of various orders, and finally we came to the conclusion that for the interval –10^{0}C …+80^{0}C the optimum fit of the B mode is made with by a 2nd order polynomial, while the C-mode is described by a 3rd order polynomial. Larger polynomial orders do not improve

Obs.	*fs [Hz]*	*R1 [ohm]*	*L1 [H]*	*C1 [F]*	*C0 [pF]*
Mod (C,3,0,1) Electr. P2+P4 in antiparallel	**7294798**	**20619**	**87,1**	**4,6 E-18**	**3,1**
Mod (B,3,0,1) Electr. P2+P4 in antiparallel	7955660	22523	70,2	6,8 E-18	3,1
Mod (C,3,1,0) Electr. P1+P3 in antiparallel	7291262	38749	58,2	8,2 E-18	2,7
Mod (B,3,1,0) Electr. P1+P3 in antiparallel	**7972292**	**28324**	**68,3**	**5,8 E-18**	**2,7**

significantly the correlation coefficient SD, but only complicate the formulas by adding extra terms difficult to handle by 8-bit microcontroller systems for example.

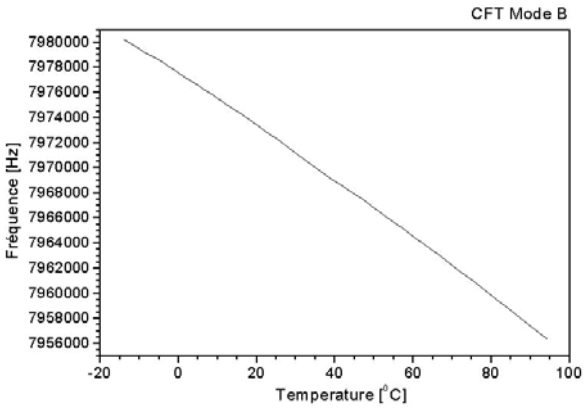

Figure 6. Frequency – temperature characteristic f_B = f (t) of B-mode.

Mode (B,3,1,0). Polynomial Regression for CFTM2B:
Y = A + B1*X + B2*X^2

Parameter	Value	Error
A	7,97756E6	7,137
B1	-203,1257	0,48741
B2	-0,22721	0,00663

R-Square(COD)	SD	N	P
0,99997	36,17484	81	<0.0001

The curves are expressed by the following equations:

$f_B = f_{B0} + b_1 t + b_2 t^2$ and

$f_C = f_{C0} + c_1 t + c_2 t^2 + c_3 t^3$,

where t is the temperature and:

$f_{B0} = 7977560$; $b_1 = -203{,}126$; $b_2 = -0{,}22721$;

$f_{C0} = 7294625{,}6$; $c_1 = 10{,}0365$; $c_2 = -0{,}11365$; $c_3 = 0.0003541$.

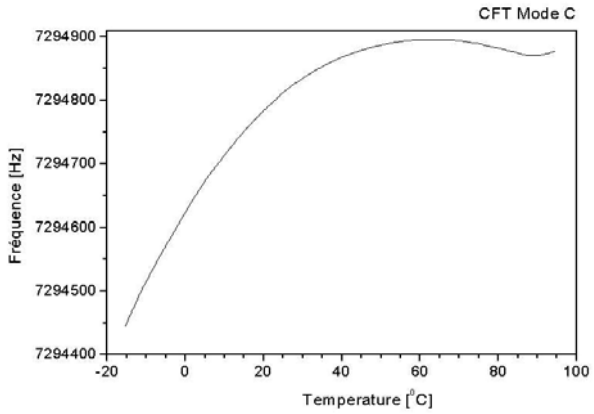

Figure 6. Frequency – temperature characteristic f_C = f (t) of the C-mode.

Mode (B,3,1,0). Polynomial Regression for CFTM2B:
Y = A + B1*X + B2*X^2

Parameter	Value	Error
A	7,97756E6	7,137
B1	-203,1257	0,48741
B2	-0,22721	0,00663

R-Square(COD)	SD	N	P
0,99997	36,17484	81	<0.0001

2.3 Force to frequency experimental characteristic

Diametral force sensitivity was previously investigated [4],[5] and is known to depend of the azimuth angle (figure 1). For a given direction the force-frequency dependence is linear up to 95% of the crushing load.

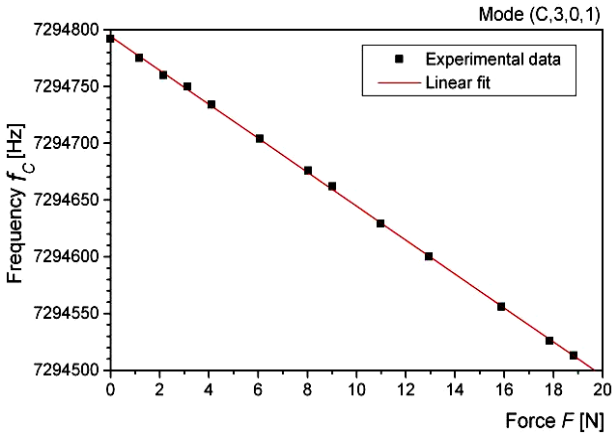

Figure 8. Linear frequency to force characteristic of C-mode f_C = f (F) at ψ_a = 75 ^{0}azymouth angle.

As seen in figure 3.c, we tested the resonant structure under compressional diametral force by adding calibrated weights on the mobile superior blade. Nonlinearities of frequency response in figure 8 are not caused by the sensor, but especially by the bearing frictions.

It has been experimentally investigated the frequency coefficient of force sensitivity for different force orientations [1]. Finally, it has been recorded that for an azimuth angle ψ_a = 75 ^{0} the force sensitivity of the C mode is almost maximum while the force sensitivity of the B mode is insignificant.

Linear Fit for Frequency-Force Characteristic:
Y = A + B * X

Parameter	Value	Error
A	7294794,04	0,84218
B	-14,94751	0,08037

For the azimuth angle ψ_a = 75 ^{0} the experimental sensitivity coefficients of the C and B modes are:

$$S_{FC} = \frac{\Delta f_C}{F} = -14{,}95 \text{ Hz/N}$$

$$S_{FB} = \frac{\Delta f_B}{\Delta F} \cong 0 << S_{FC}$$

2.4 Transfer equations of force and temperature and related errors formulae

Finally we get the set of equations relying the frequencies to nonelectric quantities temperature and force.

$$\Delta f_B = f_B - f_{B0} = b_1 t + b_2 t^2 + S_{FB} F \qquad \text{(x)}$$

$$\Delta f_C = f_C - f_{C0} = c_1 t + c_2 t^2 + c_3 t^3 + S_{FC} F$$

From equation (x) we get the temperature value based on f_B frequency and $S_{FB}F$ factor.

$$t = \frac{-b_1 - \sqrt{b_1^2 - 4b_2 \cdot (S_{FB} F - \Delta f_B)}}{2b_2}$$

Ignoring $S_{FB}F$ factor the set of equations become:

$$\Delta f_B = b_1 t + b_2 t^2$$

$$\Delta f_C = c_1 t + c_2 t^2 + c_3 t^3 + S_{FC} F$$

With the solution:

$$t = \frac{-b_1 - \sqrt{b_1^2 + 4b_2 \cdot \Delta f_B}}{2b_2}, \text{ and}$$

$$F = \frac{1}{S_{FC}} \left(\Delta f_C - c_1 t - c_2 t^2 - c_3 t^3 \right)$$

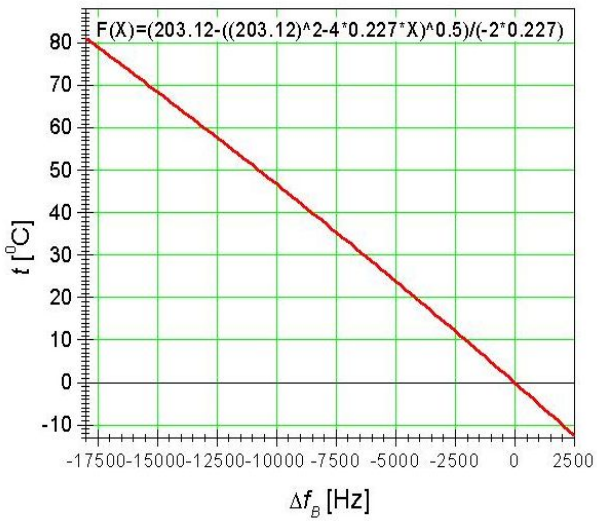

Figure 9. Temperature to frequency transfer function where $S_{FB}F$ factor is neglected.

We computed the ε_t si ε_F relative error:

$$\varepsilon_t = \frac{b_1(\varepsilon_{b_2} - \varepsilon_{b_1}) - \varepsilon_{b_2} A - \frac{1}{A}\left(b_1^2 \varepsilon_{b_1} + 2(b_2 \varepsilon_{b_2} + \varepsilon_{\Delta f_B} \Delta f_B)\right)}{-b_1 + A}$$

where $A = \sqrt{b_1^2 + 4 b_2 \Delta f_B}$

Force relative error is then given by formula:

$$\varepsilon_F = \frac{f_C \varepsilon_{f_C} - c_1 t \varepsilon_{c_1} - c_2 t^2 \varepsilon_{c_2} - c_3 t^3 \varepsilon_{c_3} + t\varepsilon_t \cdot \left(c_1 + 2c_2 t + 3c_3 t^2\right)}{f_C - c_1 t - c_2 t^2 - c_3 t^3}$$

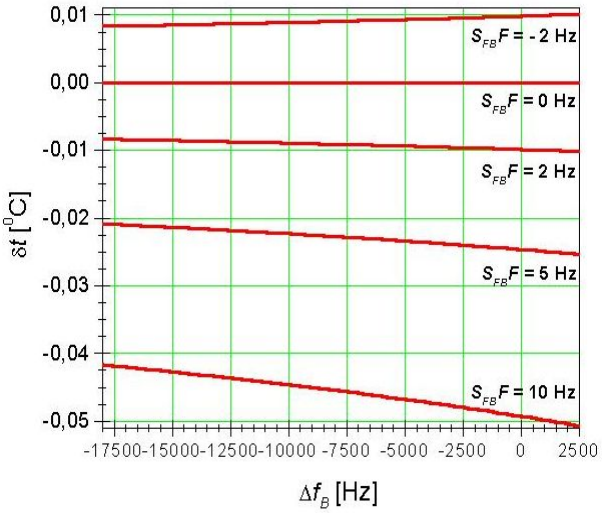

Figure 10. Temperature absolute error caused by neglecting $S_{FB}F$ factor

Ignoring $S_{FB}F$ factor simplifies the microcontroller algorithm of extracting F and t values. However, as seen in figure 10, errors arise. For example, an error of $\pm 2^0$ in ψ_a positioning angle will lead to force relative deviations of ±0.3%, which is still acceptable.

2. QUARTZ THERMOSENSITIVE (QT) RESONATORS

Several types of bulk acoustic wave QT resonators were designed and prototyped [7], intending progressive miniaturization [8] and improved electrical characteristics, starting from classical resonator shapes featuring circular plates with deposited electrodes and ending up with rectangular strip resonators. The strip resonators offer reduced plate size (up to 5.0 x 2.034 x 0.084 mm) and fit into TC39 enclosures for classical 32kHz wristwatch quartz. The thickness-shear main mode of QT resonators vibrates at 29 MHz. The NLC-cut (theta = -31°30') of this family of resonators allows a temperature sensitivity of 1200 Hz/K. The resolution reach 0.0001K depending on the stability of the reference clock as well as the local conditions, which permits to utilize these sensors as secondary temperature references. Also, these resonators are very suitable for cryogenic temperature sensing (up to liquid helium boiling point of 4.2 K).

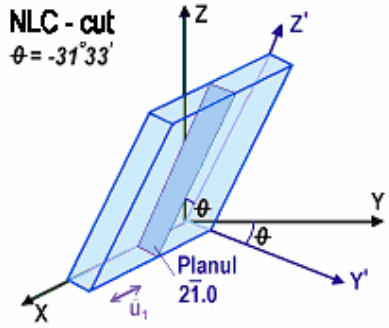

Figure 11. The NLC-Cut in quartz.

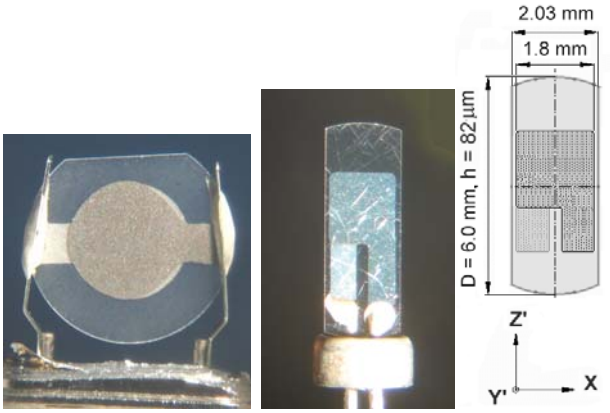

Figure 12. QT samples: classic round plate and reduced size strip resonator

As seen in the figure below, frequency – to – temperature characteristic of QT resonators is not linear in wide ranges. In fact room temperature sensitivity (1200 Hz/K) decreases nonlinearily with the temperature dropping about 700 Hz/K at liquid nitrogen boiling point, or to only about 2 Hz/K at helium point (however, at that temperature all traditional measurement techniques are unusable)

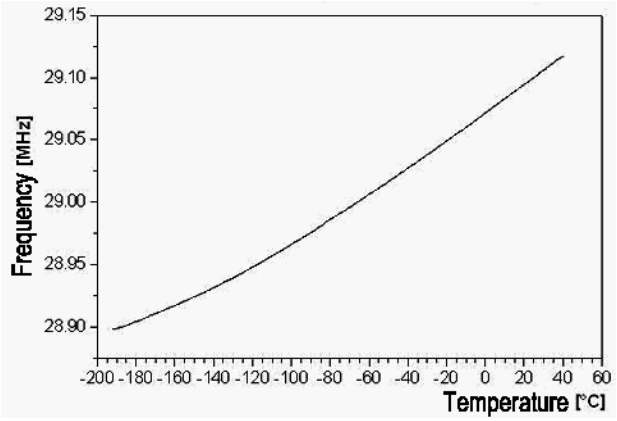

Figure 13. Typical frequency – to – temperature characteristic of QT sensors from liquid nitrogen up to room temperature

3. DISTRIBUTED ELECTRONIC SYSTEM

Main components of the electronic system of measurement are based on master-slaves open architecture. Precise time base is obtained from a 20 MHz reference temperature compensated oscillator (TCXO). This component is critical, since the accuracy of the system is dependant on the stability of the frequency reference; the system two types of conversions are possible: locally or master requested. TCXO reference can provide clock to one individual or several slave microcontrollers
In figure 14 the slave system is configured for multi-electrode (ME) resonators, with three counters enabled (two oscillators plus TCXO reference)

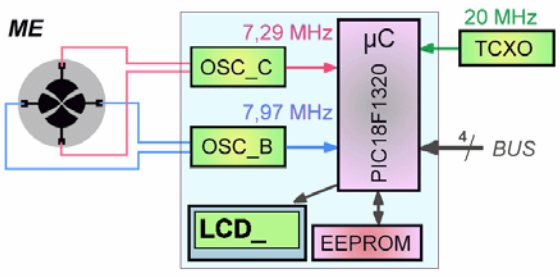

Figure 14. Slave microcontroller architecture configured for multielectrode resonator

Quartz QT sensors require one electronic oscillator. The same system can interface equally this type of resonator, by enabling two of its internal counters.

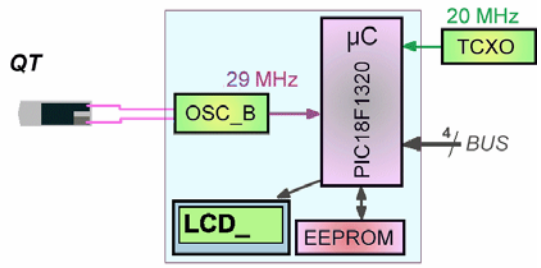

Figure 14. Slave microcontroller architecture configured for quartz thermosensitive resonator

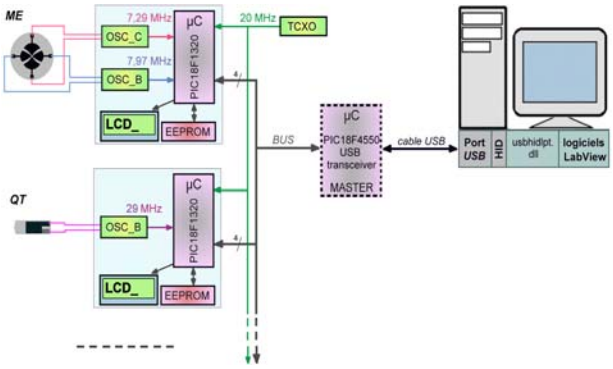

Figure 16. Architecture of measurement system where the reference TCXO signal is connected to the bus.

3.1 Slave microcontroller schematic

Slave microcontroller schematic contains the following components:

- Two independent oscillators connected to the multielectrode resonator
- A microcontroller with three 16 bit integrated counters (PIC18F1320)
- A EEPROM memory designed to store conversion parameters and recorded data
- A synchronous serial interface bus to communicate with the master controller (for adjusting the registers and for delivering the data).
- An “in circuit debug” (ICD2) interface for programming and debugging the mic-rocontroller.
- A common 16x2 LCD display.
- Two touch buttons for menu browsing.

The electronic schematic is not complicated, provided the need to offer a low cost-device. The

TCXO interrupts the microcontroller at precise time periods (1/8 s, 1s or 8s). The frequencies are afterwards converted into temperature and/or force according to formulas presented in the 2nd paragraph and stored tables. Converted values are displayed to the LCD display (figures 18-19). The information may also be sent to a master (e.g. the computer) via the serial bus.

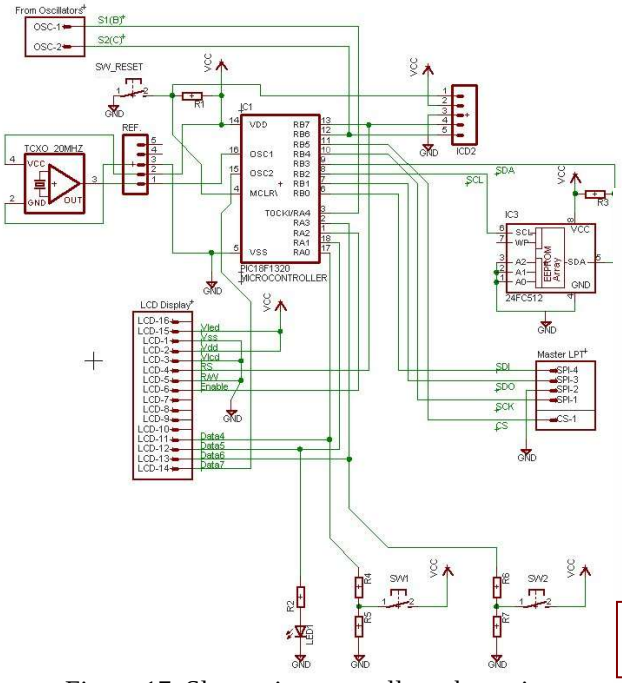

Figure 17. Slave microcontroller schematic connected to TCXO.

Figure 18. System local conversion (ME sensor)

Figure 19. System local conversion (QT sensor) LCD display captures.

3.1 Master microcontroller schematic and interface

Master microcontroller (18F4550) schematic has the following features as seen in figure 14:

- A synchronous serial interface bus to communicate with the slave controllers.
- An LCD display and a keypad port
- Four signaling state LEDs
- Four channels 8-bit analog-to-digital inputs to connect to TC1047A temperature sensors, HIH3610 humidity sensor and MPX4115 pressure sensor (used for calibration purposes).

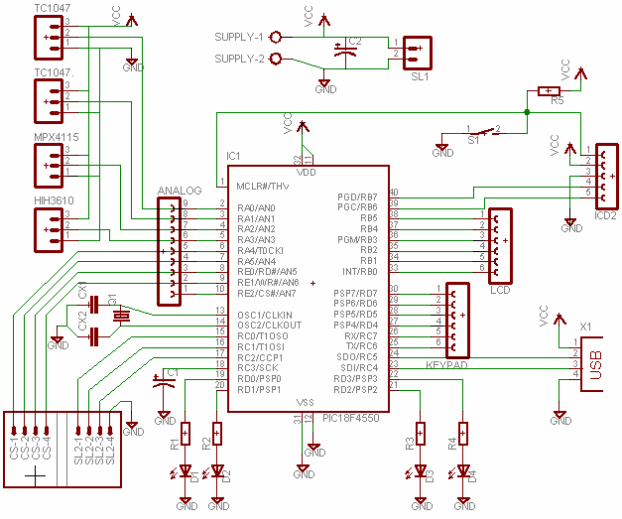

Figure 20. Master microcontroller schematic

The microcontroller is able to handle USB communication. The computer interface was done using USB-HID (human interface device) protocol.

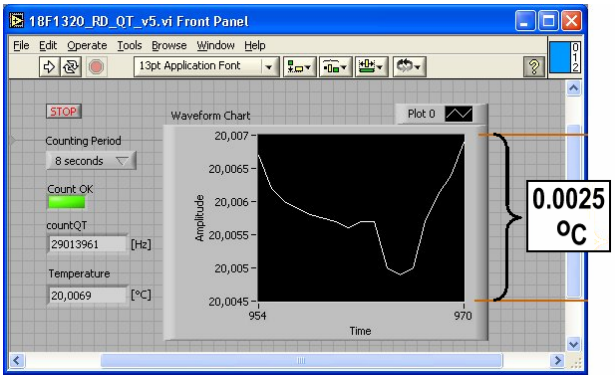

Figure 21. Labview primary acquisition interface interface.

The resolution of the QT resonators reach 0.0001 ^{0}C. A temperature flow chart at maximum resolution may be noticed in figure 21. Counting period was 8 seconds. The Y axis had a 0.0025 ^{0}C range.

The resolution of a multielectrode self compensated sensor is 0.06 N and it ranges up to 200 N.

4 CONCLUSIONS

Frequency output resonators intended for non-electrical quantities offer a better noise immunity than classical voltage output sensors, being suitable for remote or distributed systems, especially on harsh environments.

Nowadays, since microcontrollers [9] and development tools [10] are very accessible and powerful, containing for instance integrated counters and bus interfaces, the design of low cost high precision measurement systems for resonant sensors is straightforward, as seen in te present paper. Further developments consist to improve the microcontroller-distributed algorithm and to realize a performing virtual instrumentation interface under National Instruments LabView [11].

Acknowledgments

Main author would like to acknowledge the EU project QxSens - *Multi-channel measurement and control system based on resonant piezoelectric crystal sensors* (G6RD-CT-2002-00648) for allowing research funding as well as the prolific collaboration with professors Roger Bourquin and Bernard Dulmet from FEMTO-ST Department LCEP/ENSMM, Besançon, France, as well as professor Lozan Spassov from AELab, ISSP-BAS, Sofia - Bulgaria.

REFERENCES

[1] A. Ivan, R. Bourquin, B. Dulmet, *Dual mode, multiple electrodes quartz sensor*, Proc. IEEE – Int. Ultrasonics Symposium (2005)

[2] J. Zelenka, *Piezoelectric Resonators and their Applications*, Czechoslovak Academy of Sciences, Prague (1986)

[3] R. Bourquin, J.J. Boy, B. Dulmet, *SC-cut resonator with reduction of B-mode electrical response*, Proc. IEEE Int. Frequency Control Symp. (1997)

[4] R. Bourquin, B.Dulmet, *Force Sensitivity of trapped energy vibrations in a contoured resonator*, 41st Ann.Freq.Cont.Symp. p. 289-294 (1987)

[5] B.Dulmet, R.Bourquin, N.Shibanova, *Frequency-output force sensor using a multimode doubly rotated quartz sensor*, Sensors and Actuators, A 48, p.109-116 (1995)

[6] G. Genestier, *Application de la topographie par rayons X a l'etude des modes de vibration dans un resonateur a onde de volume*, These de doctorat l'Université de Franche-Comté (1982)

[7] L. Spassov et. al., *Investigations of electrical parameters and mode patterns of NLC quartz resonator at low temperature*, 18th EFTF (European Forum of Time and Frequency) Proc. (2004)

[8] B. Dulmet et al, *Design of a new miniature resonant temperature sensor in NLC-cut of quartz*,19th EFTF Proc. (2005)

[9] ***, *PIC18Fxxxx Data Sheet*, Microchip Technology Inc., (2004)

[10] ***, MPLAB IDE 7.*20 Users Manual*, Microchip Technology Inc., (2005)

[11] ***, *Labview 7 Users Manual*, National Instruments, (2002)